

*gkElectronic Supplementary Information for*

**Defect-rich CeO<sub>2</sub> in a hollow carbon matrix engineered from a microporous organic platform:  
a hydroxide-assisted high performance pseudocapacitive material**

*Hyeon Seok Jeong,<sup>a‡</sup> Chang Wan Kang,<sup>a‡</sup> Yoon Myung,<sup>b</sup> Sang Moon Lee,<sup>c</sup> Hae Jin Kim,<sup>c</sup>  
and Seung Uk Son<sup>\*a</sup>*

<sup>a</sup> Department of Chemistry, Sungkyunkwan University, Suwon 16419, Korea

E-mail: sson@skku.edu

<sup>b</sup> Dongnam Regional Division, Korea Institute of Industrial Technology, Busan 46938, Korea

<sup>c</sup> Korea Basic Science Institute, Daejeon 34133, Korea

**Fig. S1.** SEM and TEM images of (a, d) H-MOP, (b, e) H-MOP/CeO<sub>2</sub>-4, and (c, f) P-CeO<sub>2</sub>.

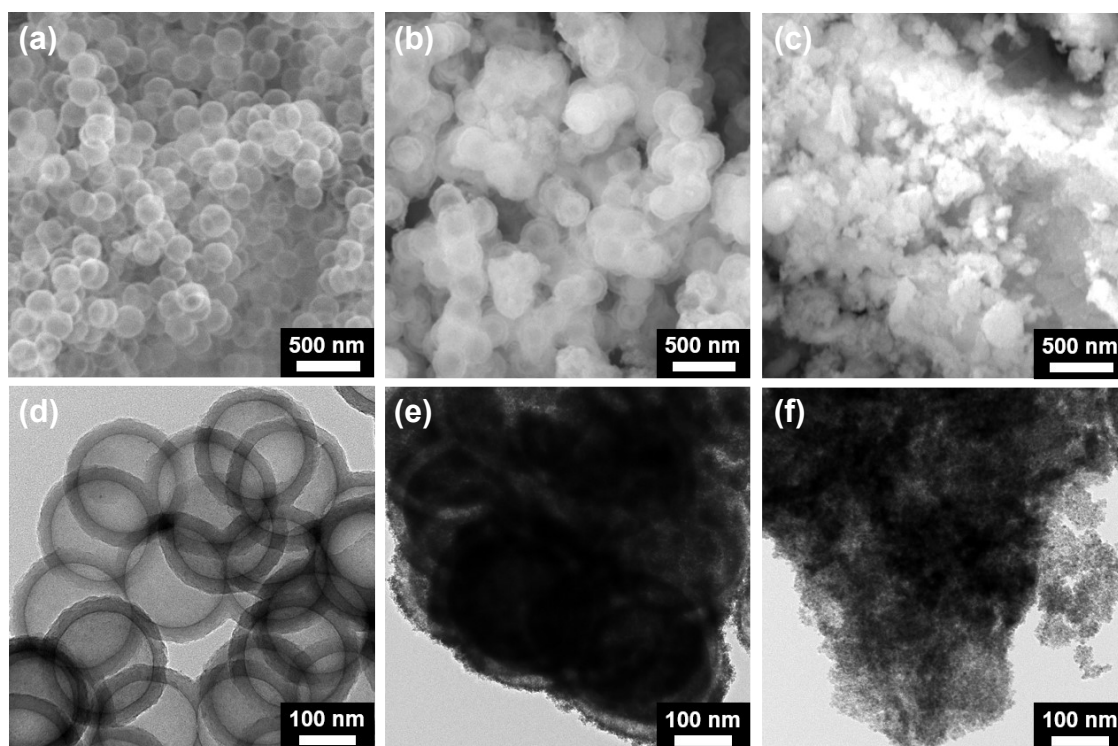


**Fig. S2.** Characterization data of H-MOP/CeO<sub>2</sub>-4 and H-C/CeO<sub>2</sub>-4: (a) N<sub>2</sub> adsorption-desorption isotherm curves (77K) and a pore size-distribution diagrams (based on the DFT method) and (b) PXRD patterns. Also, refer to Table S1 in the ESI.

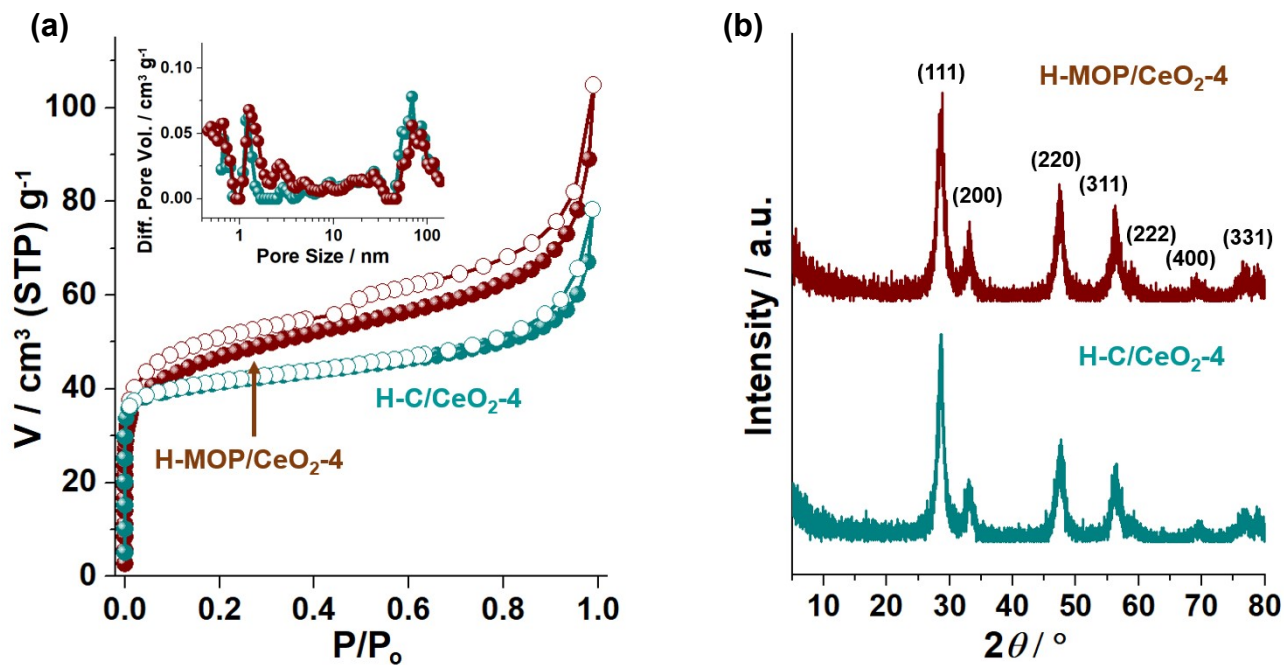


**Fig. S3.** N<sub>2</sub> adsorption-desorption isotherm curves (at 77K) and a pore size-distribution diagrams (based on the DFT method) of P-CeO<sub>2</sub> and CeO<sub>2</sub>. Also, refer to Table S1 in the ESI.

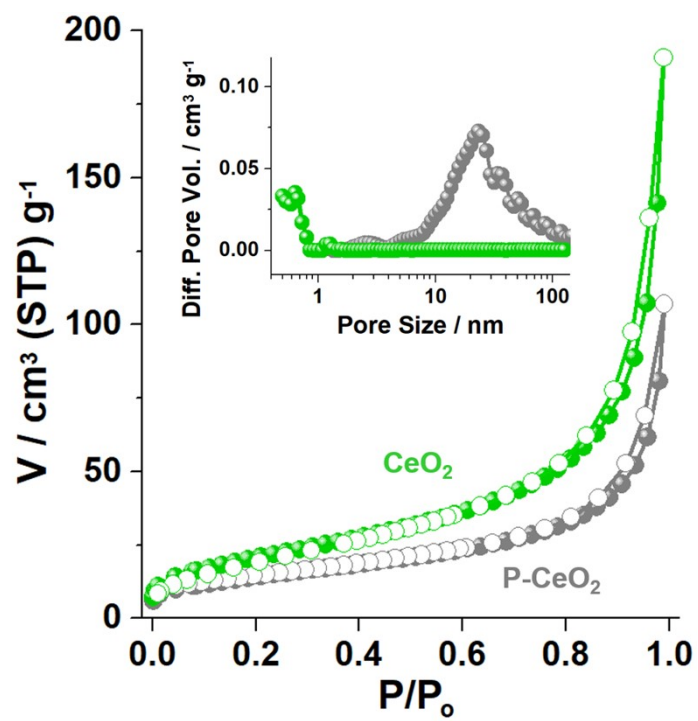
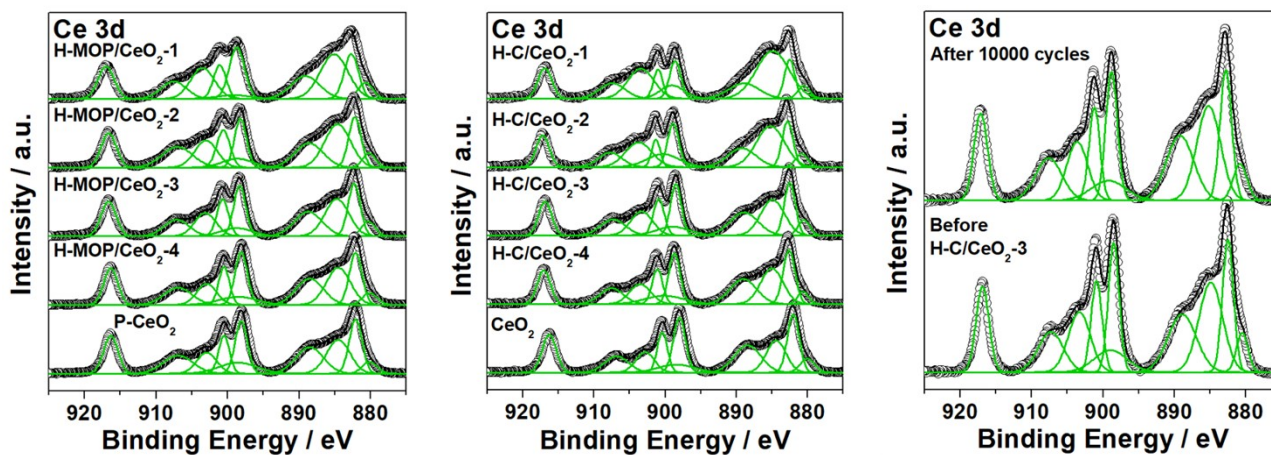


**Fig. S4.** Quantitative analysis of  $\text{Ce}^{3+}/(\text{Ce}^{3+} + \text{Ce}^{4+})$  through the XPS Ce 3d orbital peak fitting (refer to K. I. Maslakov, Y. A. Teterin, A. J. Popel, A. Y. Teterin, K. E. Ivanov, S. N. Kalmykov, V. G. Petrov and I. Farman, *Appl. Surf. Sci.* 2018, **448**, 154-162 and Y. Zhou, J. M. Perket and J. Zhou, *J. Phys. Chem. C* 2010, **114**, 11853-11860.)



Materials	$\text{Ce}^{3+}/(\text{Ce}^{3+} + \text{Ce}^{4+})$
H-MOP/CeO <sub>2</sub> -1	0.40
H-MOP/CeO <sub>2</sub> -2	0.38
H-MOP/CeO <sub>2</sub> -3	0.36
H-MOP/CeO <sub>2</sub> -4	0.34
P-CeO <sub>2</sub>	0.33
H-C/CeO <sub>2</sub> -1	0.54
H-C/CeO <sub>2</sub> -2	0.49
H-C/CeO <sub>2</sub> -3	0.38
H-C/CeO <sub>2</sub> -3 (after 10000 cycles)	0.36
H-C/CeO <sub>2</sub> -4	0.35
CeO <sub>2</sub>	0.30

Fig. S5. TGA curves of H-MOP and H-MOP/CeO<sub>2</sub>.

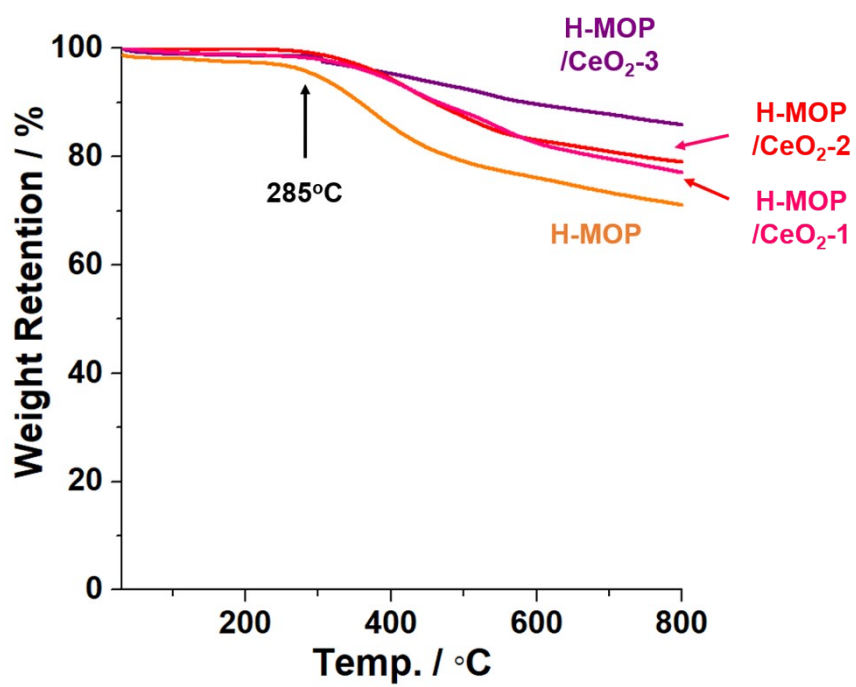


**Fig. S6.** SEM images of H-C, H-C/CeO<sub>2</sub>, and CeO<sub>2</sub>.

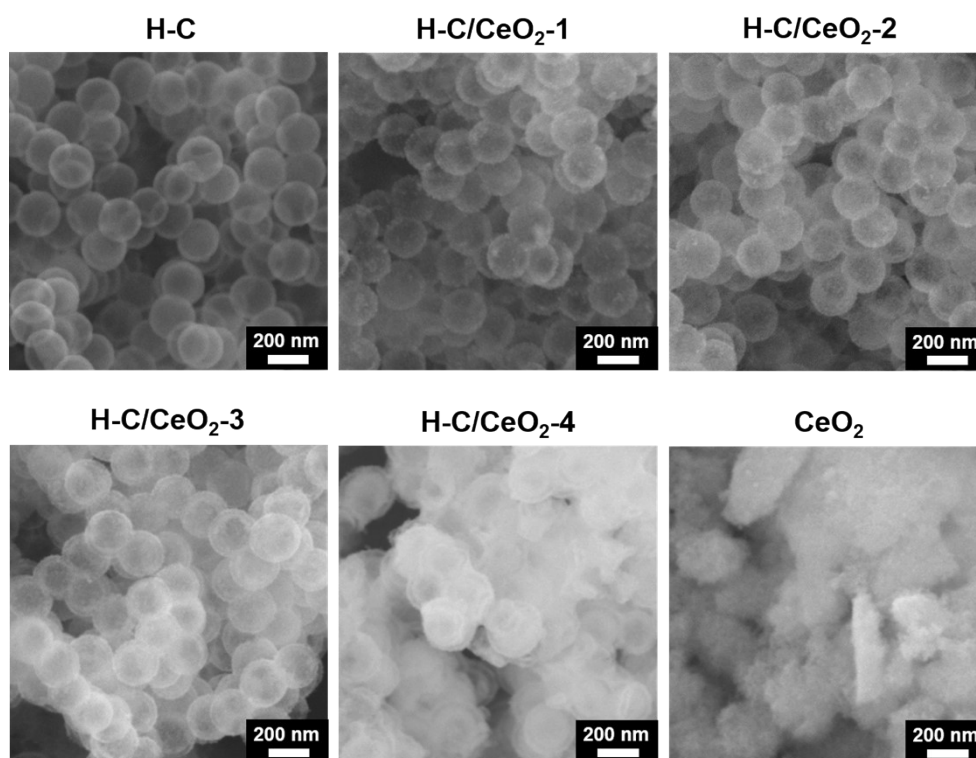


**Fig. S7.** (a) HR-TEM and (b) EDS-elemental mapping images of H-C/CeO<sub>2</sub>-3.

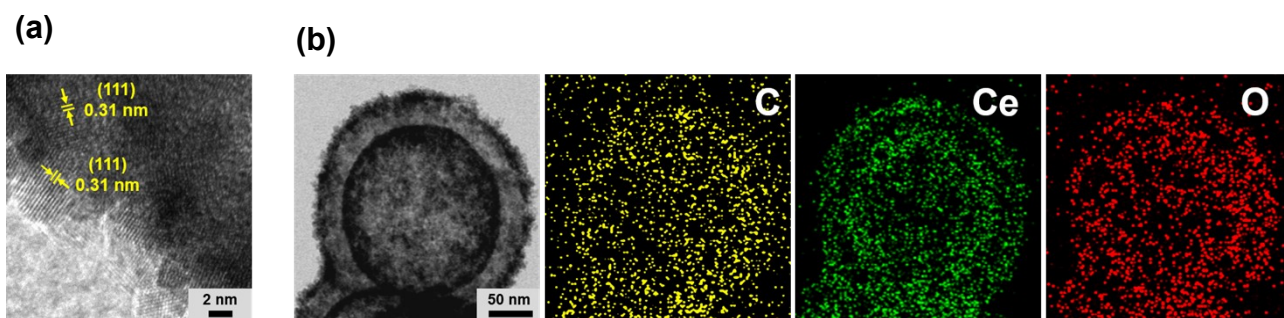


**Fig. S8.** EPR spectra of H-C, H-C/CeO<sub>2</sub>, and CeO<sub>2</sub> (a modulation frequency of 100 kHz, RT).

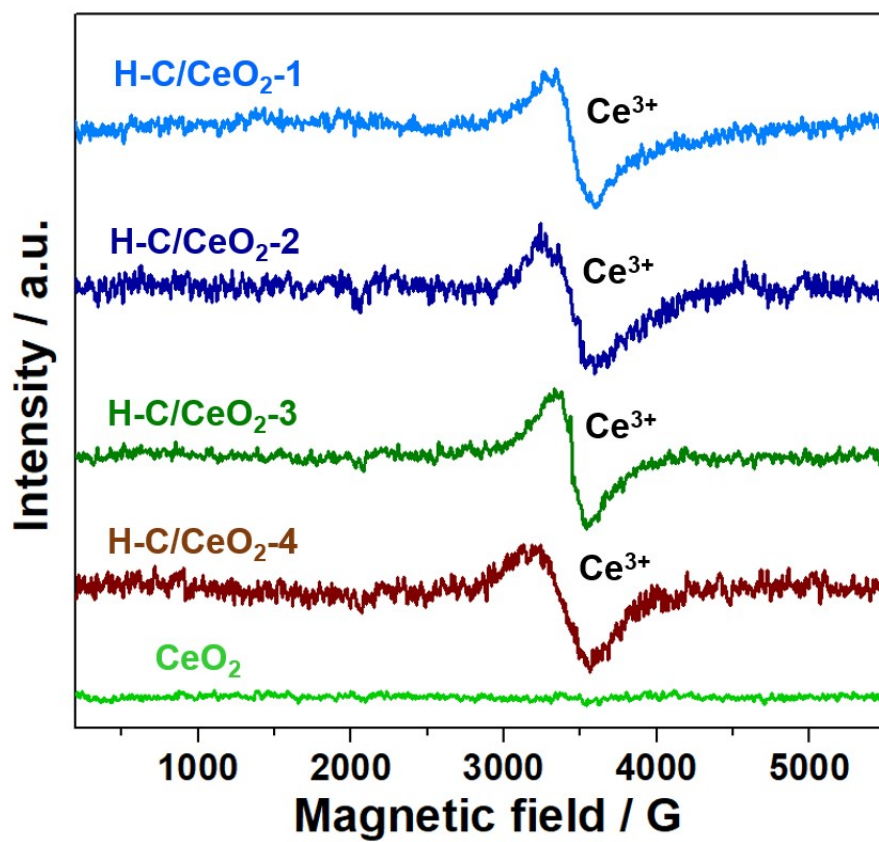




Fig. S9. Scan rate-dependent cyclic voltammograms of H-C, H-C/CeO<sub>2</sub>, and CeO<sub>2</sub>.

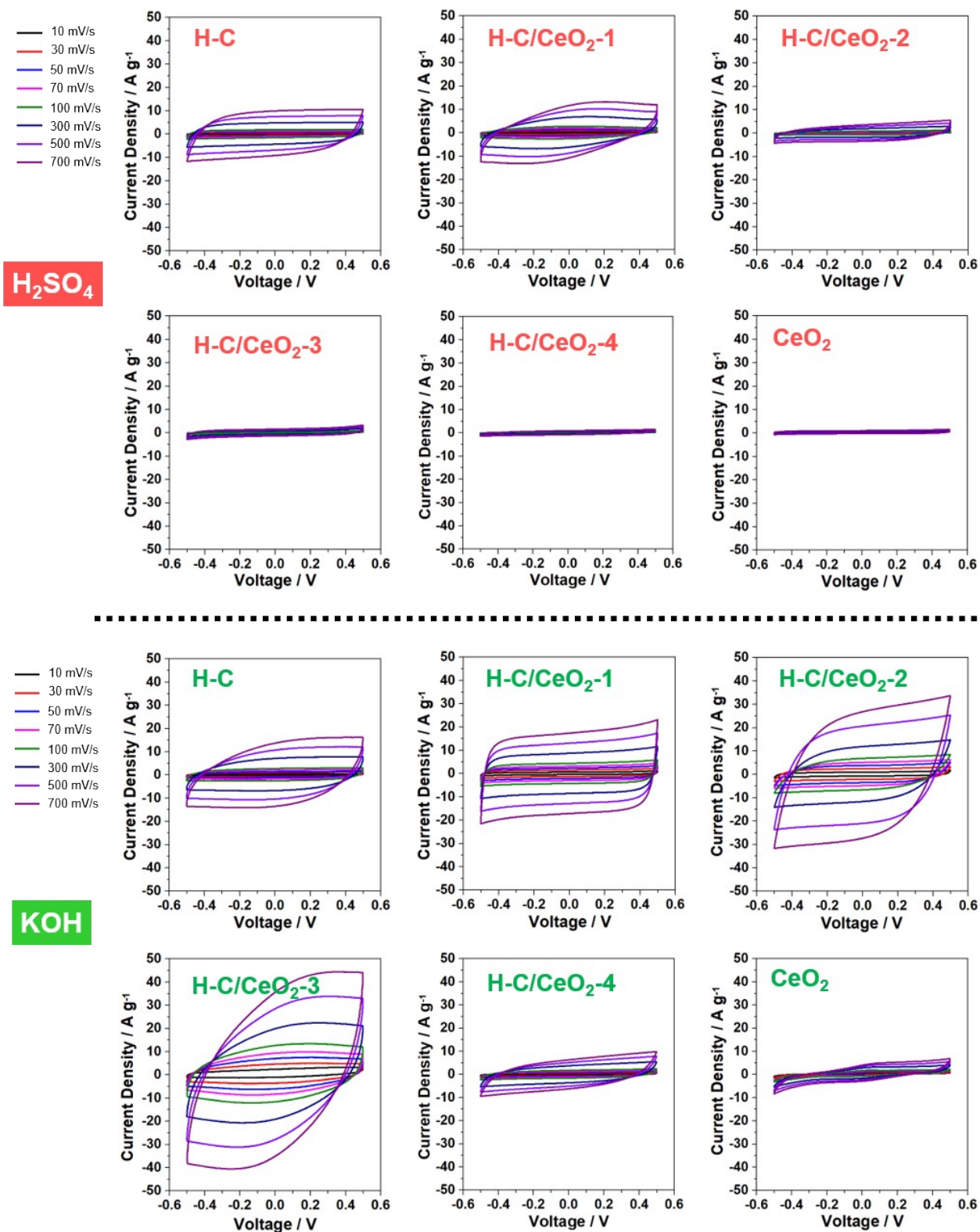
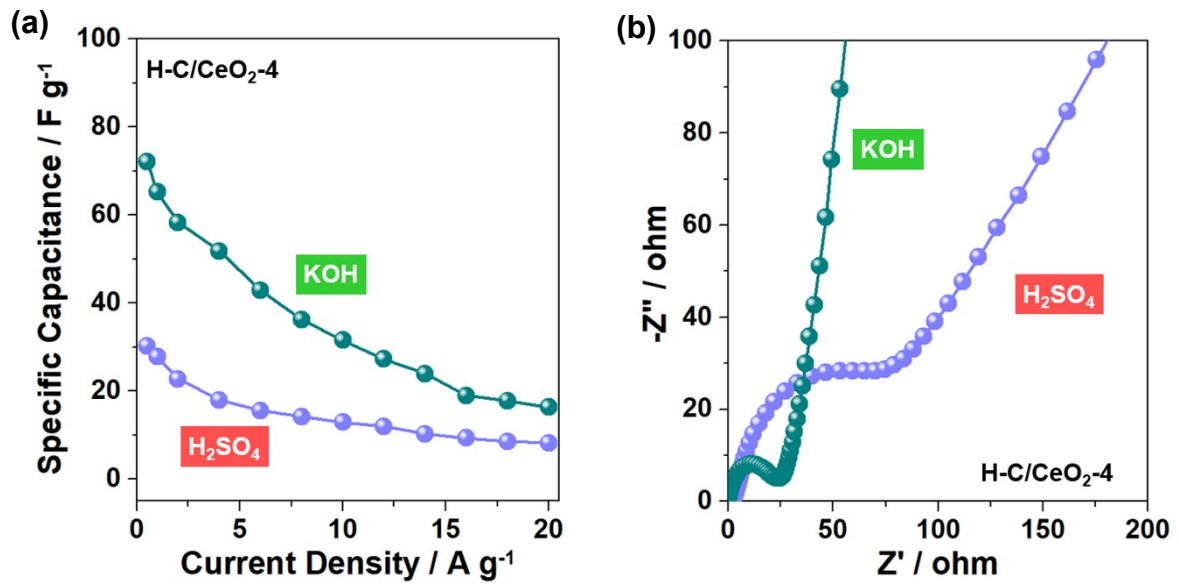
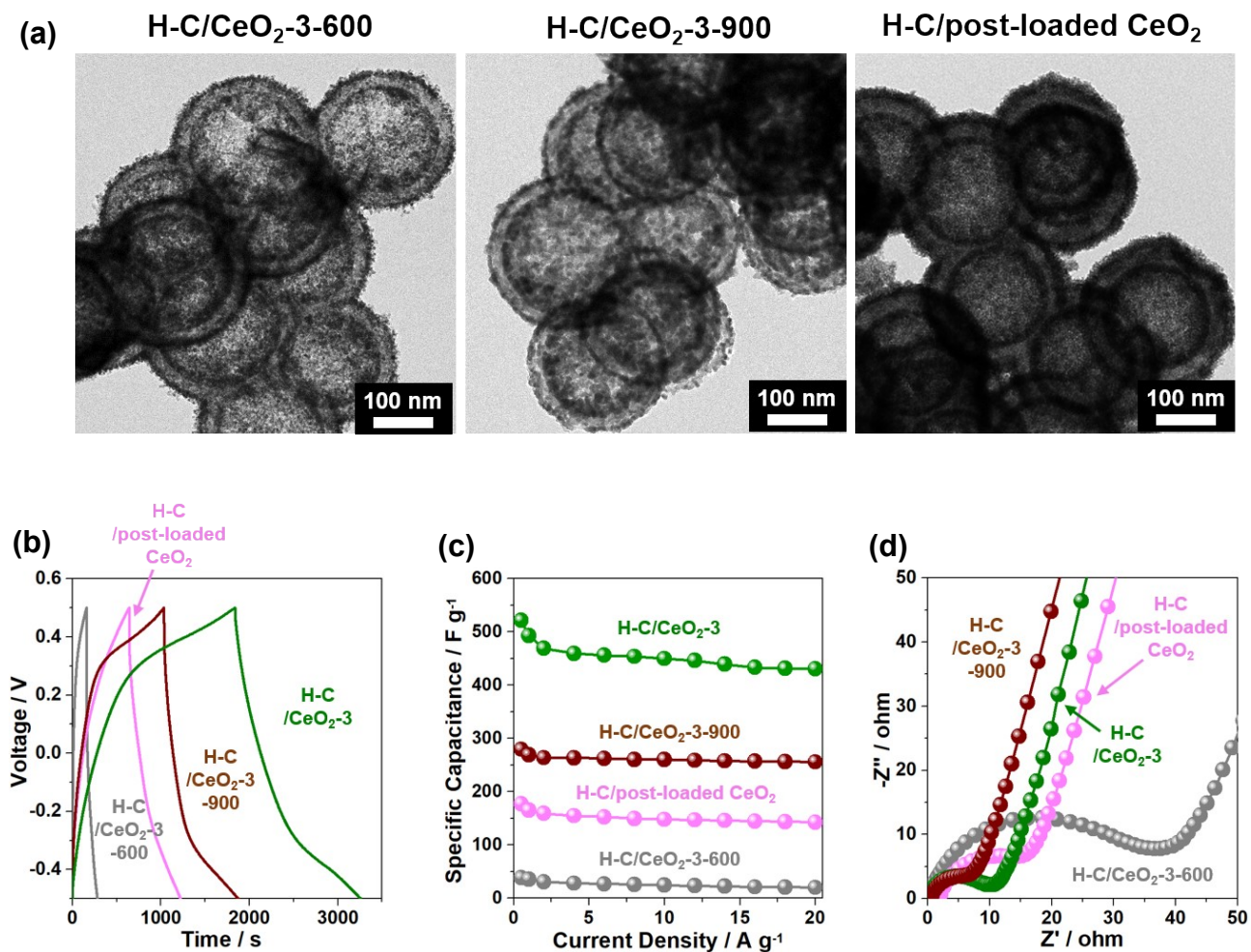


Fig. S10. Electrochemical performance of H-C/CeO<sub>2</sub>-4: (a) Rate performance and (b) Nyquist plots.



**Fig. S11.** (a) TEM images, (b) charge-discharge profiles, (c) rate performance, and (d) Nyquist plots of H-C/CeO<sub>2</sub>-3-600, H-C/CeO<sub>2</sub>-3-900, and H-C/post-loaded CeO<sub>2</sub>. The H-C/CeO<sub>2</sub>-3-600 and H-C/CeO<sub>2</sub>-3-900 were prepared by the heat-treatment of H-MOP/CeO<sub>2</sub>-3 in a furnace under argon for 4 h at 600 and 900°C, respectively. The H-C/post-loaded CeO<sub>2</sub>(57wt%) was prepared by the synthetic procedures applied for H-MOP/CeO<sub>2</sub>-3 using the H-C instead of H-MOP.



**Fig. S12.** TEM images of H-C/CeO<sub>2</sub>-3 retrieved after 10000 cycles.

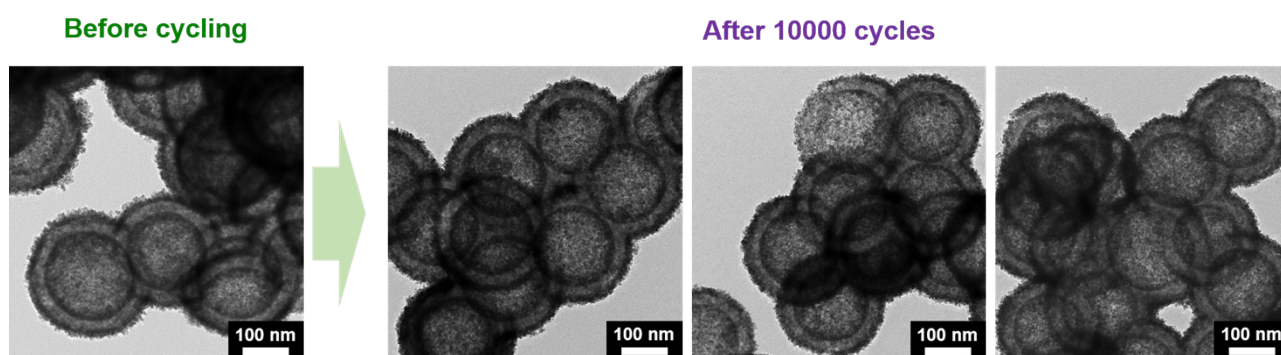


**Table S1.** Physical and electrochemical properties of H-MOP, H-MOP/CeO<sub>2</sub>, P-CeO<sub>2</sub>, H-C, H-C/CeO<sub>2</sub>, and CeO<sub>2</sub>.

Entry	Materials	$S_{\text{BET}}^{\text{a}}$ (m <sup>2</sup> /g)	$V_{\text{mic}}^{\text{b}}$ (cm <sup>3</sup> /g)	Specific Capacitance (F/g) <sup>c</sup>		
				0.5 A/g	1 A/g	10 A/g
1	H-MOP	745	0.24	-	-	-
2	H-MOP/CeO <sub>2</sub> -1	534	0.17	-	-	-
3	H-MOP/CeO <sub>2</sub> -2	403	0.12	-	-	-
4	H-MOP/CeO <sub>2</sub> -3	282	0.08	-	-	-
5	H-MOP/CeO <sub>2</sub> -4	152	0.04	-	-	-
6	P-CeO <sub>2</sub>	54	0.00	-	-	-
7	H-C	1017	0.32	195	184	153
8	H-C/CeO <sub>2</sub> -1	537	0.17	296	262	213
9	H-C/CeO <sub>2</sub> -2	425	0.16	415	378	349
10	H-C/CeO <sub>2</sub> -3	279	0.10	527	504	458
11	H-C/CeO <sub>2</sub> -4	159	0.05	72	65	31
12	CeO <sub>2</sub>	73	0.00	4.5	4.3	2.0

<sup>a</sup> Surface areas based on BET theory. <sup>b</sup> Micropore volumes based on t-plot. <sup>c</sup> The values in aqueous 6 M KOH electrolyte.

**Table S2.** Summarized energy storage performance of the recent carbonized CMP and CeO<sub>2</sub>-based electrode materials.

Entry	Materials	Types of materials	Capacitance (F/g)						Measurement type	Ref.	
			0.1 A/g	0.2 A/g	0.5 A/g	1 A/g	2 A/g	5 A/g			10 A/g
1	N3-CMP-1	Carbonized CMP	175			164			149	three electrode	1
2	G-TEPA-TPA-C	Carbonized CMP		268						two electrode	2
3	NPCM-1	Carbonized CMP	264							two electrode	3
4	H-NCB-900	Carbonized CMP				286			224	two electrode	4
5	CeO <sub>2</sub> /graphene	CeO <sub>2</sub> /C composites				208				three electrode	5
6	CeO <sub>2</sub> /graphene	CeO <sub>2</sub> /C composites					185			three electrode	6
7	MnO <sub>2</sub> /CeO <sub>2</sub>	Doped CeO <sub>2</sub> materials			274.3	265.6		236.2		three electrode	7
8	CeO <sub>2</sub> /graphene	CeO <sub>2</sub> /C composites				86.5				two electrode	8
9	CeO <sub>2</sub> /CNT	CeO <sub>2</sub> /C composites				455.7	289.7			three electrode	9
10	Co-CeO <sub>2</sub> /RGO	CeO <sub>2</sub> /C composites				298				three electrode	10
11	Porous CeO <sub>2</sub>	CeO <sub>2</sub> nanomaterials				134.6		116.2	109.5	three electrode	11
12	CeO <sub>2</sub> nanocubes	CeO <sub>2</sub> nanomaterials						88.71		three electrode	12
13	PANI/rGO/CeO <sub>2</sub>	CeO <sub>2</sub> /C composites				115.3			81.2	three electrode	13
14	Hollow CeO <sub>2</sub> /MWCNT	CeO <sub>2</sub> /C composites			450.5				389.7	three electrode	14
15	Cr-CeO <sub>2</sub>	Doped CeO <sub>2</sub> materials			328					three electrode	15
16	CeO <sub>2</sub> nanocrystals	CeO <sub>2</sub> nanomaterials				339.5			161	three electrode	16
17	H-C/CeO <sub>2</sub> -3	CeO <sub>2</sub> /C composites			527	493			458 440	two electrode	This work

- 1 J. -S. M. Lee, T. -H. Wu, B. M. Alston, M. E. Briggs, T. Hasell, C. C. Hu and A. I. Cooper, *J. Mater. Chem. A* 2016, **4**, 7665-7673.
- 2 K. Yuan, P. Guo-Wang, T. Hu, L. Shi, R. Zeng, M. Forster, T. Pichler, Y. Chen and U. Scherf, *Chem. Mater.* 2015, **27**, 7403-7411.
- 3 Y. Xu, S. Wu, S. Ren, J. Ji, Y. Yue and J. Shen, *RSC Adv.* 2017, **7**, 32496-32501.
- 4 J. Lee, J. Choi, D. Kang, Y. Myung, S. M. Lee, H. J. Kim, Y. -J. Ko, S. -K. Kim and S. U. Son, *ACS Sustainable Chem. Eng* 2018, **6**, 3525-3532.
- 5 Y. Wang, C. X. Guo, J. Liu, T. Chen, H. Yang and C. M. Li, *Dalton Trans.* 2011, **40**, 6388-6391.
- 6 A. S. Dezfuli, M. R. Ganjali, H. R. Naderi and P. Norouzi, *RSC Adv.* 2015, **5**, 46050-46058.
- 7 H. Zhang, J. Gu, J. Tong, Y. Hu, B. Guan, B. Hu, J. Zhao and C. Wang, *Chem. Eng. J.* 2016, **286**, 139-149.
- 8 Y. Tao, L. Ruiyi, Z. Haiyan and L. Zaijun, *Mater. Res. Bull.* 2016, **78**, 163-171.
- 9 D. Deng, N. Chen, Y. Li, X. Xing, X. Liu, X. Xiao and Y. Wang, *Physica E* 2017, **86**, 284-291.
- 10 S. Parwaiz, K. Bhunia, A. K. Das, M. M. Khan and D. Pradhan, *J. Phys. Chem. C* 2017, **121**, 20165-20176.
- 11 K. Prasanna, P. Santhoshkumar, Y. N. Jo, I. N. Sivagami, S. H. Kang, Y. C. Joe and C. W. Lee, *Appl. Surf. Sci.* 2018, **449**, 454-460.
- 12 M. P. Chavhan, S. Som and C. -H. Lu, *Mater. Lett.* 2019, **257**, 126598.
- 13 A. Jeyaranjan, T. S. Sakthivel, C. J. Neal and S. Seal, *Carbon* 2019, **151**, 192-202.
- 14 Z. -J. Sun, H. Ge, S. Zhu, X. -M. Cao, X. Guo, Z. -H. Xiu, Z. -H. Huang, H. Li, T. Ma and X. -M. Song, *J. Mater. Chem. A* 2019, **7**, 12008-12017.
- 15 S. Ghosh, K. Anbalagan, U. N. Kumar, T. Thomas and G. R. Rao, *Appl. Mater. Today* 2020, **21**, 100872.
- 16 X. Hao, S. Zhang, Y. Xu, L. Tang, K. Inoue, M. Saito, S. Ma, C. Chen, B. Xu, T. Adschiri and Y. Ikuhara, *Nanoscale* 2021, **13**, 10393-10401.